Geotechnical Aspects of Underground Construction in Soft Ground, Kastner, Emeriault, Dias, Guilloux (eds)
© 2002 Spécifique, Lyon. ISBN 2-9510416-3-2

Numerical analysis of diaphragm wall construction and subsequent pit excavation in clayey ground

R. Schaefer & T. Triantafyllidis
Insitute for soil mechanics and foundation engineering
Ruhr-Universität Bochum, Germany

ABSTRACT: In order to investigate the influence of the construction process on the deformation of a diaphragm wall, a two dimensional finite element model is presented. The construction of the wall is simulated first and wall movements due to the subsequent pit excavation are compared with those of a conventional calculation assuming the wall as wished-in-place. During the construction process the earth pressure at rest and hydrostatic pore water pressure are changed adjacent to the wall affecting the calculated wall deflections. However, the influence of construction depends on the desigend retaining system. Whereas a cantilever or anchored wall shows greater horizontal movements mainly the prop force increases considering a strutted wall.

1 INTRODUCTION

In order to ensure serviceability of retaining walls and to protect nearby structures it is important to minimize ground and wall movements during the pit excavation. The FEM is a powerful tool to calculate the ground and wall deformation, but the comparison between the in-situ values and numerical results shows frequently great differences.

One reason is that FEM-calculations normally do not consider significant aspects, like the construction of the retaining wall, which affect the behaviour of the ground. As initial condition, conventional computation choose the earth pressure at rest acting on the retaining wall prior to excavation.

In fact the process of the wall construction itself influences the properties of the adjacent ground and changes earth pressure conditions. In order to predict deformations acurately at the stage of pit excavation, it is important to consider the change of initial conditions due to the construction process of the wall.

2 NUMERICAL MODEL

In order to investigate the influence of retaining wall construction on later wall movements, a two dimensional finite element model of a diaphragm wall in clayey ground is generated. Two calculations are performed respectively, the first choosing the earth pressure at rest as initial condition and the second simulating the construction of the retaining wall prior to pit exvavation. Three different systems are considered (Fig. 1). The ground water table is 2 m below the ground level, but due to capillarity the ground was assumed to be fully saturated.

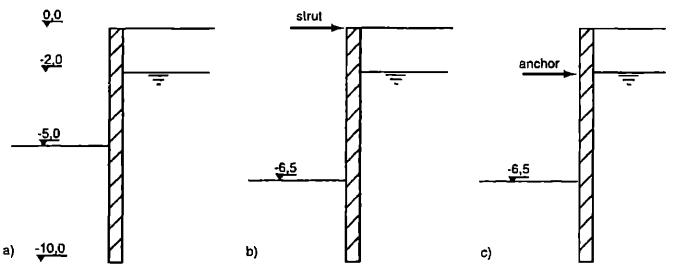

Figure 1. Calculated systems: a) cantilever, b) strutted, c) anchored

The homogenous overconsolidated soil deposit is described by the following visco-hypoplastic constitutive equation (Niemunis ,1996).

$$\dot{\mathbf{T}} = \mathcal{L}(\mathbf{T},e) : (\mathbf{D} - \mathbf{D}^v) \tag{1}$$

$$\mathbf{D}^v = - \frac{\mathbf{B}}{\|\mathbf{B}\|} \cdot \gamma \left(\frac{1}{OCR} \right)^{1/I_v} \tag{2}$$

The stiffness $\mathcal{L}$, which depends on the actual stress state $\mathbf{T}$ and the void ratio e, and the direction $\mathbf{B}$ of plastic strain rate $\mathbf{D}^v$ results from hypoplasticity. Further state variables and parameters are described in table 1.

Table 1. Soil parameters used in the analysis

Soil parameter	
φ_c – residual friction angle	22.5^0
C_c – compression index	0.086
C_s – swelling index	0.012
I_v – index of viscoity	0.02

$\dot{\gamma}$ - reference deformation rate	$2{,}78 \cdot 10^{-6}$ s^{-1}
γ – bulk unit weight	17.7 kN/m^3
k – permeability	10^{-8} m/s
K_0 – earth pressure coefficient at rest	0.8

state variable	
OCR – over-consolidation-ratio	2
e_{eo} – reference void ratio	0.984
T – actual stress	
$\dot{\mathbf{T}}$ – stress rate	
e – actual void ratio	
D – total strain rate	
$\mathbf{D}^v$ – viscous strain rate	

The small-strain stiffness of the soil owing to changes of the strain path is regarded by a further state variable called intergranular strain (Niemunis, 2002). Supposing that no cracking of concrete will occur during pit excavation, the diaphragm wall is described by a linear-elastic continuum with a Young's modulus of 30000 MN/m^2 and a Possion ratio of 0.2. The earth pressure at rest is calculated according to Mayne and Kulhawy (1982):

$$K_0 = (1 - \sin \varphi_{crit}) \cdot OCR^{\sin \varphi_{crit}} \quad (3)$$

The first numerical model is generated which assumes the retaining wall wished-in-place (wip) neglecting the construction process of the wall. The earth pressure at rest is chosen acting on the wall prior to pit excavation. The excavation of the pit is simulated by removing the finite elements in front of the wall step by step. In the case of the cantilever wall the soil is excavated up to a depth of 5 m in order to guarantee overall stability. The propped pits are excavated to a depth of 6.5 m with a remaining embedment of 3.5 m. In contrast to the strut at the top of the retaining wall, which is constructed at the beginning of the excavation process, the anchor 2 m below ground level is installed after the excavation has reached a depth of 3 m. Both, the strut and the anchor, are simulated by springs with stiffnesses corresponding to the real conditions. The preload force of the anchor results from horizontal equilibrium to 150 kN/m. The soil-structure-interaction is described by a yield stress τ_{max}, which can be transmitted between the retaining wall and the adjacent soil. In correspondence with Bjerrum (1973), τ_{max} is adopted to

$$\tau_{max} = \alpha \cdot c_u \quad (4)$$

incorporating the undrained shear strength c_u and an adhesion coefficient α. Generally α is set to 1.0 for normally consolidated and 0.3 - 0.5 for overconsolidated soil deposits. During the present calculations, an adhesion coefficient of $\alpha = 0.5$ has been chosen.

The second numerical model is generated in order to simulate the construction process of the diaphragm wall prior to the excavation sequence (cps = construction process simulated). In a first step earth pressure at rest is initialized in the FE-model according to equation (3). The finite elements inside the trench are removed and the open trench walls are supported by a distributed load representing the hydrostatic pressure of the slurry (Fig. 2a). The bulk unit weight of the slurry is set to 10.3 kN/m^3. Subsequently, pouring the trench with concrete is modeled by placing additional finite elements into the trench (Fig. 2b). In contrast to the slurry pressure, the pressure of fresh concrete is not hydrostatic over the depth of the trench (DiBiagio and Roti, 1972, Lings, Ng and Nash, 1994). Accordingly, the applied pressure in the model corresponds to hydrostatic conditions with $\gamma_{concrete} = 23.5$ kN/m^3 up to a critical depth $h_{crit} = 4$ m. At greater depth than h_{crit} below surface level of the concrete, the fresh concrete pressure increases with a rate given by 70 % of the bulk unit weight. The development of the stiffness of fresh concrete (Fig. 2c) is considered by a suitable evolution of the Young's modulus and the Poisson ratio (Fig. 3).

During the second step of the calculation the excavation of the pit is simulated by removing the respective elements (Fig. 2d).

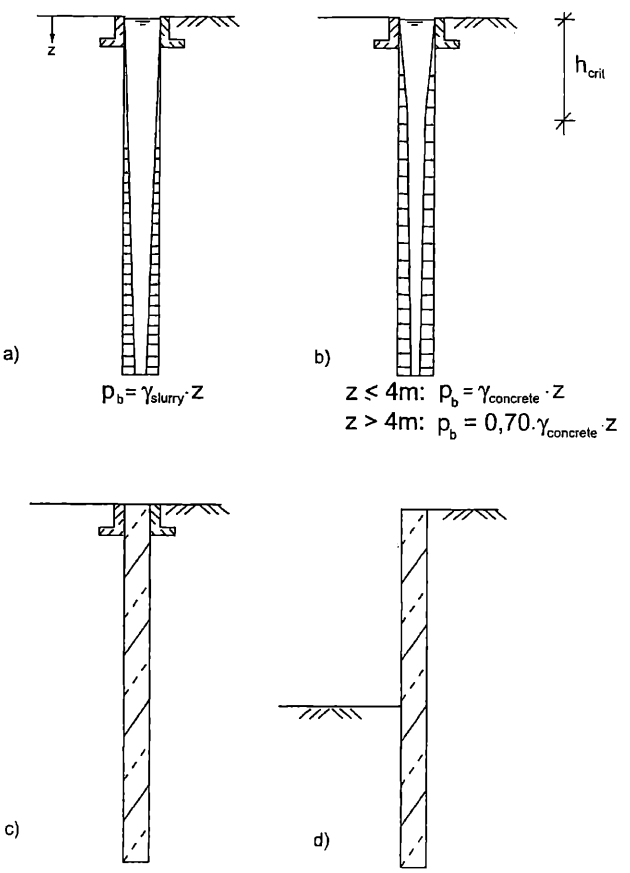

Figure 2. Construction sequence: a) excavation of the panel with slurry support, b) pouring with tremie pipes, c) curing of the concrete (28d), d) excavation of the pit

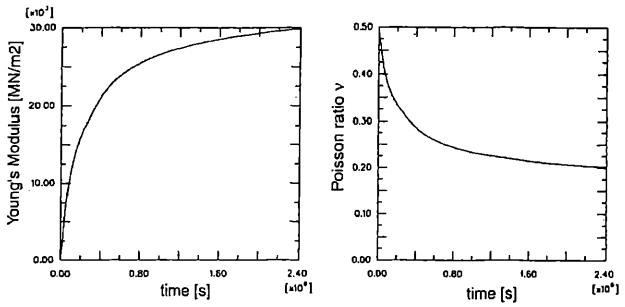

Figure 3. Development of stiffness of fresh concrete (Reinhardt, 2001)

3 NUMERICAL RESULTS

3.1 Stress conditions

Figure 4 shows the effective horizontal stress σ_h' and Figure 5 the total pore pressure u adjacent to the diaphragm wall panel during different construction steps of the retaining wall. The steps comprise the initial pressure at rest conditions, the slurry support of the excavated trench and the subsequent filling of fresh concrete. Additionally, the stresses are presented after the concrete has cured (28 days).

During the excavation of the panel, the effective stress σ_h' increases behind the guide wall and below the toe of the trench due to a vertical arching effect. The resulting earth pressure corresponds to an earth pressure coefficient $\sigma_h' / \sigma_v' = 1.45$ and 1.27 respectively whereas in the middle part of the excavated panel, σ' remains nearly unchanged.

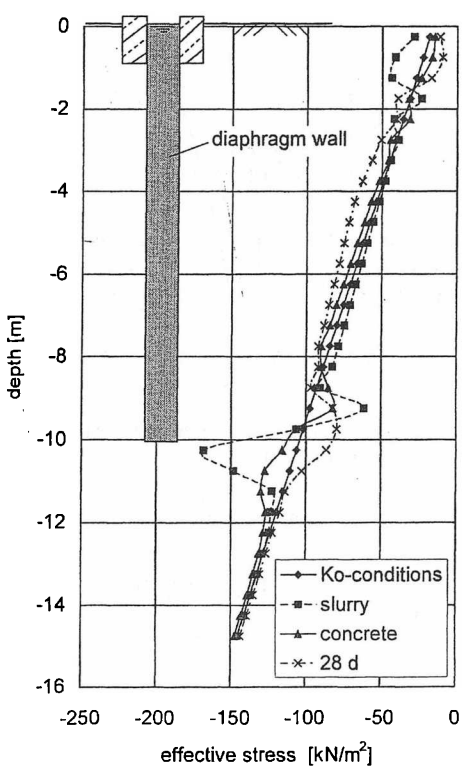

Figure 4. Effective stress σ_h' adjacent to the wall

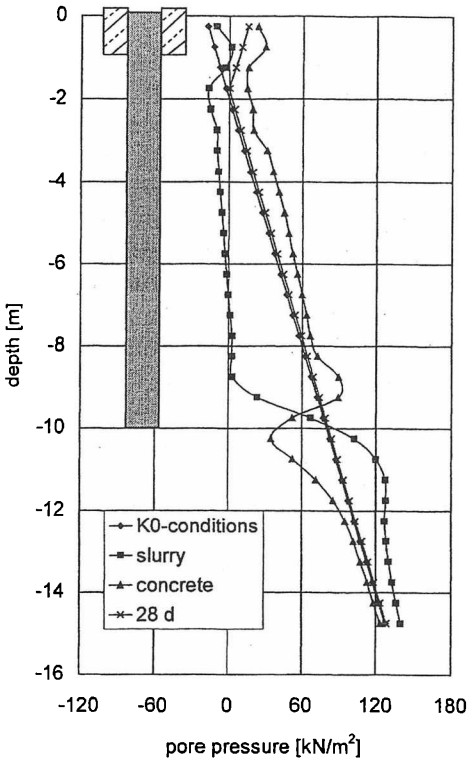

Figure 5. Pore pressure u adjacent to the wall

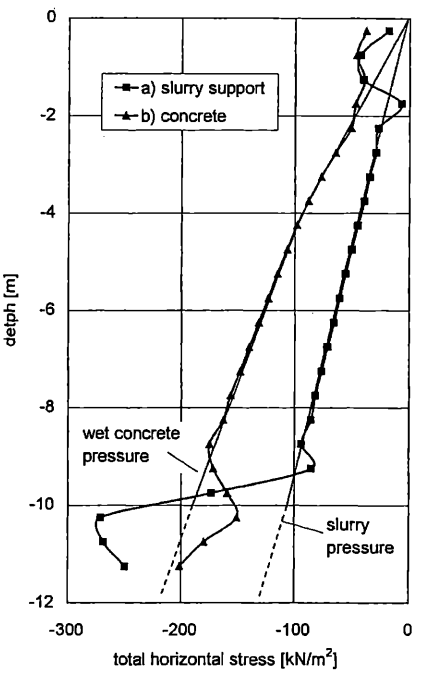

Figure 6. Distribution of total horizontal stress during the construction process of the diaphragm wall panel

The vertical arching is also clearly shown in the total stress distribution presented in Fig. 6. To avoid the oscillating gradient of σ_h' above the toe of the wall (Fig. 4) a finer finite-element-mesh should be generated here. During the concreting sequence of the panel, the vertical arching is fully reversed which has already been observed by Gourvenec and Powrie (1999). The earth pressure behind the guide walls

and below the toe of the wall is reduced to less than the initial conditions.

The development of the pore pressure u is comparable to σ_h'. In the first step excess pore pressure arises behind the guide walls and below the excavated trench whereas u decreases and becomes negative in the middle part of the panel owing to the inward movement of trench under slurry support. During the second step of construction, the pore pressure increases due to the wet concrete pressure and exceeds the hydrostatic conditions behind the panel (Fig. 5). After a time period of 28 days, the excess pore water has totally dissipated and the effective horizontal stress equilibrates the concrete pressure now.

Considering the total horizontal stress $\sigma = \sigma' + u$ adjacent to the trench, σ drops from the initial conditions to the bentonite pressure first and subsequently increases to the wet concrete pressure during the construction process (Fig. 6).

3.2 Wall movements

The deflected wall profiles due to pit excavation are shown in Fig. 7a and 8a,b under totally undrained conditions directly after the end of excavation (short-term behaviour). Respectively the calculated wall movements of the two models are plotted, the first neglecting (wip) and the second simulating the construction process of the diaphragm wall (cps). The horizontal movements s have been scaled with the depth of the excavation pit H. Furthermore, the long-term wall movements of the cantilever beam are plotted in Fig. 7b including the excess pore water dissipation during a time period of one year.

Considering the wall movements of the different systems after pit excavation, the deflections of the cantilever are greatest. As it was expected, the largest deflections were calculated at the top of the wall. The anchored and the strutted diaphragm walls show a maximum horizontal movement at the bottom of the excavation. Comparing the plotted results of the wip- and the cps-model, wall movements of the latter are obviously greater, independent of the system under consideration. However, the difference between the curves, which can be described as construction-induced wall movement, seems to depend on whether the retaining wall is propped or not. Tables 2 – 5 compare the calculated wall movements at the top of the wall and at the bottom of excavation for the wip- and the cps-model. The anchor (prestressed with 150 kN/m) and the strut forces are also presented. Furthermore the total Δ and the relative δ differences between the considered values are given.

The strut at the top of the diaphragm wall provides a rigid support. The construction of the retaining wall only leads to a higher strut force of about 15 % of the conventional calculation whereas wall movements are hardly influenced. Considering the cantilever and the anchored wall, horizontal wall movements increase about 15 % and 35 % respectively due to the construction process. However, the dissipation of excess pore water does not have a significant influence. Although the total horizontal movements increase about 70 %, the difference between the wip- and the cps-model remains nearly constant (see Fig. 7).

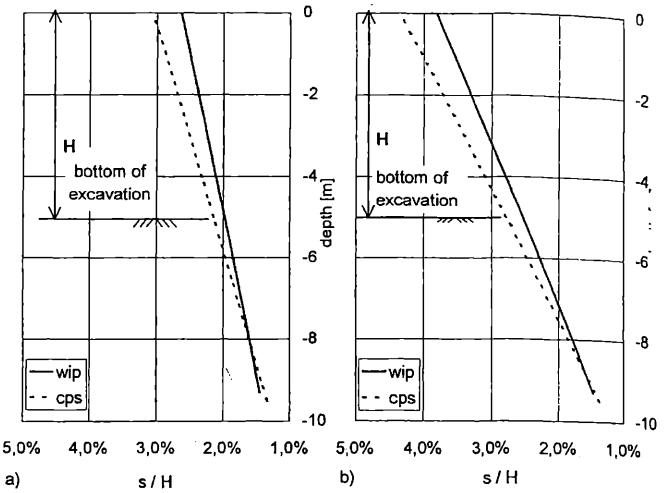

Figure 7.Wall deflection of cantilever wall, disregarding and including construction of the wall a) short term b) long term

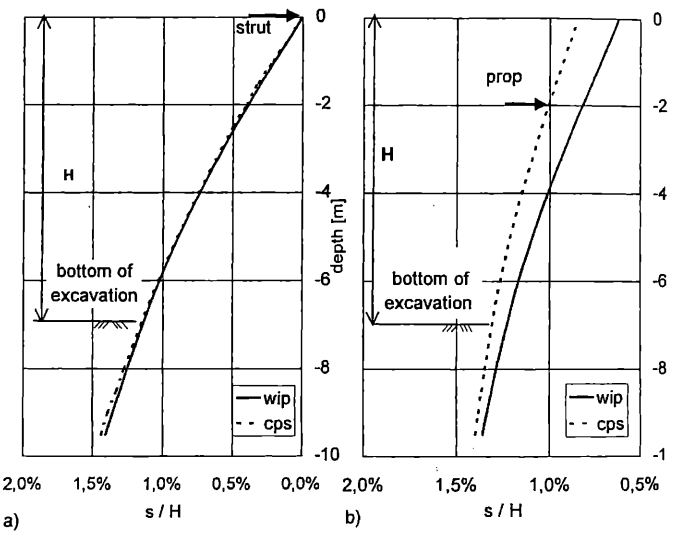

Figure 8. Wall deflection of a) strutted and b) anchored wall, disregarding and including construction of the wall

Table 2 Calculated wall movements of the cantilever wall, short-term behaviour

FE-model	top of the wall	bottom of excavation
wip	13.2 cm	9.9 cm
construction	15.3 cm	10.7 cm
Δ	2.1 cm	0.8 cm
δ	15.9 %	8.1 %

Table 3 Calculated wall movements of the cantilever wall, long-term behaviour

FE-model	top of the wall	bottom of excavation
wip	19.3 cm	12.7 cm

construction	21.8 cm	13.9 cm
Δ	2.5 cm	1.2 cm
δ	13.0 %	9.4 %

Table 4 Calculated wall movements and strut forces of the strutted wall

FE-model	top of the wall	bottom of excavation	strut force
wip	≈ 0 cm	7.1 cm	214.5 kN/m
construction		7.13 cm	245.5 kN/m
Δ	0	0.03 cm	31 kN/m
δ	0 %	0.4 %	14.5 %

Table 5 Calculated wall movements and anchor forces of the anchored wall

FE-model	top of the wall	bottom of excavation	strut force
wip	4.0 cm	7.8 cm	199.1 kN/m
construction	5.4 cm	8.4 cm	217.0 kN/m
Δ	1.4 cm	0.6 cm	18.1 kN/m
δ	35 %	7.7 %	9.1 %

4 DISCUSSION

Due to the construction process of the diaphragm wall, the total horizontal stresses σ adjacent to the wall are affected (Fig. 9). In the upper part of the retaining wall, σ increase of approximately $\Delta\sigma = 15 - 18$ % in comparison with the initial conditions at rest. The total stress distribution after construction (Fig. 6 and Fig. 9 curve b) is determined by the wet conrete pressure and less influenced by the initial pressure conditions (K_0 and pore pressure).

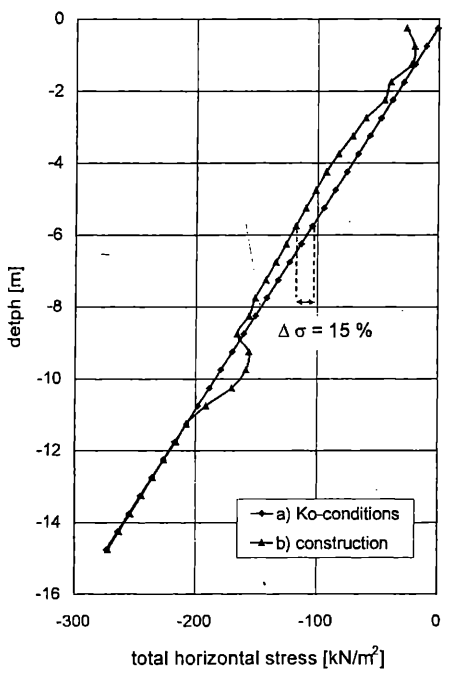

Figure 9. Total horizontal stress adjacent to the wall a) K_0-conditions, b) after the end of construction

Therefore Δσ, which indicates the difference in total stresses prior to pit excavation between the wip- and the cps-model, depends mostly on the initial stress conditions and the distribution of the fresh concrete pressure. If the concrete pressure exceeds the total pressure at rest, horizontal wall deflections due to pit excavation will increase. In the case of higher earth pressure coefficients and high ground water tables, the construction process of the wall will lead to decreasing total stresses which probably results in smaller wall deflections.

Figure 10 shows the stress path, expressed by the mean effective stress p' and the deviatoric stress q, of a finite element 1.25 m below the bottom of excavation during the construction process of the retaining wall and the subsequent pit excavation. Due to excavation of the trench under slurry support, the deviatoric stress q increases first (point 0 → point 1). However, q is reset by filling the panel with fresh concrete (point 2) and p' increases during the subsequent pouring process of the concrete (dissipation of excess pore water, point 3). Although the stress conditions at the beginning of pit excavation differ between the wip- and the cps-model (points 0 and 3), both stress paths process parallel and end at the same point after the excavation of the pit and the dissipation of excess pore pressure (point 5).

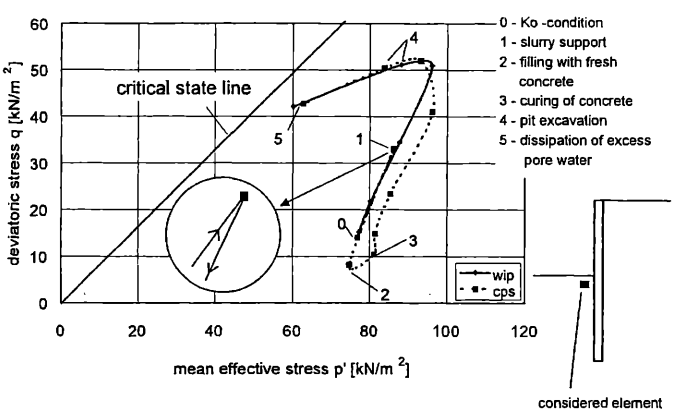

Figure 10. Stress paths during construction and excavation process

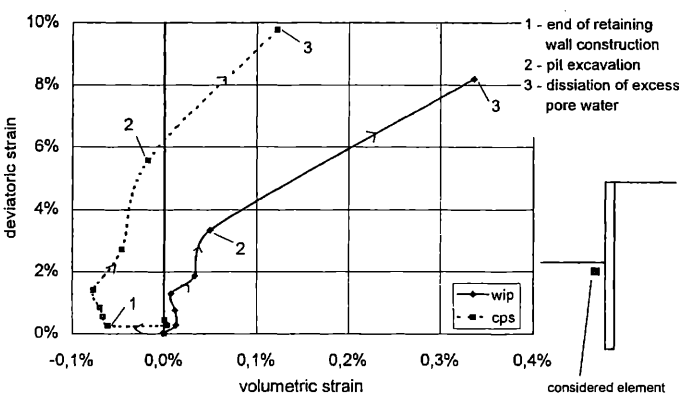

Figure 11. Strain paths during construction and excavation process

In Fig. 11 the strain paths of the same element like in Fig. 10 are plotted during the construction and the excavation process for the wip- and the cps-model. Considering the wip-model, the soil element in front of the retaining wall mainly undergoes deviatoric strains up to a value of about ε_{wip} = 8 % after the dissipation of excess pore water. On the contrary, the same element undergoes an isotropic compression during the construction of the diaphragm wall (point 1) first and the deviatoric strains go up to ε_{cps} = 9.8 % at the end of pit excavation (point 3).

The difference between the calculated deviatoric strains, which corresponds to greater wall deflections of the cps-model, mainly arises from plastic deformations because the stress paths and consequently the elastic strains are similar for both models (Fig. 10). In Fig. 12 the development of the over-consolidation-ratio (OCR) of the considered element towards the excavation depth is shown. Owing to the construction process of the diaphragm wall, the over-consolidation-ratio drops from the initial value of 2.0 to 1.976. During the subsequent pit excavation, the soil in front of the wall approaches the critical state (see. Fig.10) and OCR decreases. However, the OCR calculated by the cps-model always remains below those of the wip-model. Due to viscous strain rates $\mathbf{D}_v$ being proportional to $\approx (1/OCR)^{20}$ (see eq. 2), greater plastic soil deformations consequently arise.

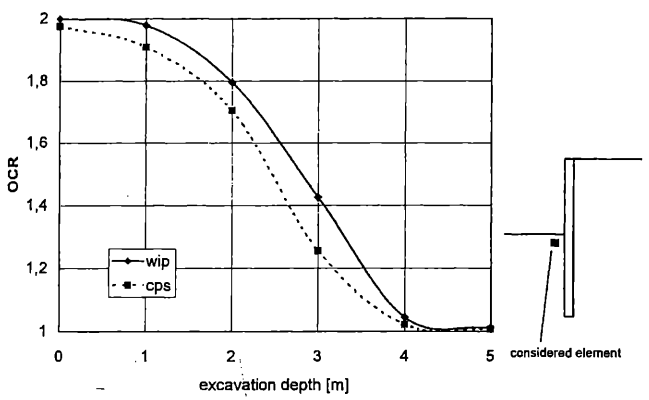

Figure 12. Over-consolidation-ratio towards excavation depth

5 CONCLUSIONS

Simulating the construction process of the diaphragm wall prior to the excavation of the pit leads to greater wall deflections and prop forces of the calculated systems. The influence mainly results from higher total pressures behind the retaining wall at the beginning of the excavation process, which are induced by the fresh concrete pressure. Obviously the difference between the concrete pressure and the total horizontal pressure at rest determines the construction influence. If the concrete pressure exceeds the total pressure at rest, greater wall deflections and prop forces are to be expected subsequent to pit excavation. However, the influence seems to be dependent on the designed retaining system. Considering strutted walls, wall deflections are hardly affected by the construction whereas the strut force increases of about 15 %. Greater horizontal wall deflections are to be expected for cantilever or anchored walls. Nevertheless, the construction of a diaphragm wall is obviously a three dimensional process and therefore a 2-D calculation can be regarded as approximation only. A three dimensional finite element model is in preparation in order to analyse the spatial earth pressure (arching) effects and different sequences of diaphragm wall panel construction.

REFERENCES

Bjerrum (1973): Problems of soil mechanics and construction on soft clays, Proc. 8th ICSM-FE Moskau, Bd. 3, p. 11

DiBiagio E., Roti J.A. (1972): Earth pressure measurement on a braced slurry-trench wall in soft clay, 5th European Conference on Soil Mechanics and Foundation Engineering, Madrid, pp. 473 – 483

Gourvenec S.M., Powrie W. (1999): Three-dimensional finite-element analysis of diaphragm wall installation, Géotechnique 49, No. 6, pp. 801 – 823

Lings M., Ng C.W.W., Nash D.F.T. (1994): The lateral pressure of wet concrete in diaphragm wall panels cast under bentonite, Proc. Instn Civ. Engrs.: Geotech. Engng 107, pp. 163 – 172

Mayne P. W., Kulhawy F. H. (1982): K_0-OCR Relationships in Soil, Journal of the Geotechnical Engineering Division, ASCE, Vol. 108, pp. 851 – 872

Niemunis A. (1996): A visco-plastic model for clay and its FE-implementation, XI Colloque Franco-Polonais en Mécanique des Sols et des Roches Appliquée Gdansk, 1996

Niemunis A.(2002): Extensions to the hypoplastic model for soils, dissertation submitted for habilitation, Gdansk, 2002

Reinhardt H.-W. (2001): Beton, Beton-Kalender 2001, Ernst & Sohn